Jurnal Ilmiah PPI-UKM
Scientific Journal of PPI-UKM
Persatuan Pelajar Indonesia
Universiti Kebangsaan Malaysia
Selangor, Malaysia

Scientific Journal of PPI-UKM

Science and Engineering

Vol. 3 No. 1
ISSN No. 2356 - 2536

The Assessment Characteristic of ZnO Material for Optical Sensing Layer Probe Using Average Scanning of FFT (ASFFT) Method

Harry Ramza[1,2*], Latifah Sarah Supian[3], Norhana Arsad[4]
Mohammad Syuhaimi Ab-Rahman[1]

[1]*SPECTRUM Technology Laboratory, Department Electrical, Electronic and System Engineering*
Faculty of Engineeering and Built Environment
Universiti Kebangsaan Malaysia, Bangi, 43600, Malaysia
Engineering Building, Telp No: +601-33716332, Fax No: +603-89216146
Email:hramza@eng.ukm.my, syuhaimi@eng.ukm.my

[2]*Department of Electrical Engineering, Faculty of Engineering*
Universitas Muhammadiyah Prof. Dr. HAMKA, Jakarta, 13830, Indonesia
Jalan Tanah Merdeka No.6B, Kampung Rambutan, Telp No. +62 21-8400941, Fax No: +62 21-87782739

[3]*Department of Electrical and Electronic Engineering, Faculty of Engineering*
Universiti Pertahanan Nasional, Kuala Lumpur, 57000, Malaysia
Bestari Building 7th floor, Kem Sungai Besi
Telp No: +603-90513400, Fax No: +603-90513472, E-mail: cawa711@gmail.com

[4]*Photonic Laboratory, Department Electrical, Electronic and System Engineering*
Faculty of Engineeering and Built Environment
Universiti Kebangsaan Malaysia, Bangi, 43600, Malaysia
Engineering Building, Telp No: +603-89216837, Fax No: +603-89216146, E-mail: norhana@eng.ukm.my

Abstract

ZnO material characterization was done to be used as optical probes from the plastic optical fiber. Characterization of ZnO materials by processing data obtained from scanning probe microscope (SPM) NTEGRA-AURA. The obtained data is in the form of images with different distance observations. It will be processed by 11 simulated images of proceeds image analysis (IA Analysis). Methodology of data processing is using average scanning Fast Fourier Transformation (ASFFT). This method consists of five characterization data processing techniques, i.e., power spectral density techniques, power spectral technique, magnitude spectrum technique, square root magnitude spectrum techniques and logarithmic spectrum techniques. The goal of average scanning FFT is determines a value of special characterization, because the result of surface morphology from SPM images cannot give exact information . Each techniques in this method will be used to see the details of each ZnO layer surface morphology of in units of frequency or frequency. The observation study of ZnO characterization is made by Atomic Force Microscopy without doing renovation materials. The treatment material as a layer probe of plastic optical fiber sensor was studied for detecting various chemical vapor and air pressure. Based on the detection method called interferometric Fabry – Perot, Plastic Optical Fiber probes will detect the changes of ZnO layer refractive index causes by environments.

Keywords: *Zinc Oxide, material assessment characteristic, layer probe, average scanning, fast fourier transform. (Accepted October 20, 2015., Published October 22, 2015).*

1. Introduction

Many different deposition techniques, as spray pyrolysis[1], impulse laser deposition[2], the sputtering method[3], deposition of MOCVD (Metal Organic Chemical Vapor Deposition) and radiation MBE (molecular beam epitaxial)[4] as well as dip coating that have been developed to prepare ZnO layer. Each method has relative advantages for certain applications.

Among them, the method of sprinkling is one of the most common techniques used for a number of advantages, such as low substrate temperature, deposition of high value, varied surfaces and perfect crystal orientation. However, the form of pressure raises serious impact on the character - mechanical properties of ZnO layer sputtering. Pressure in being a challenge to understand how the load impact, load rate, the proliferation behavior on the properties - mechanical properties of layers - layers.

*Author correspondence should be sent

ZnO is a semiconductor material group II - VI direct wide band gap (~ 3.4 eV at room temperature[5]) and have learned a few years ago. Although the use of key technical material, initially connected to the high light efficiency and the use of power electronics[6-8]. ZnO material is found widely in the cosmetics industry and is a component of antiseptic cream and lotion UV inhibitors. Currently ZnO has emerged as a leading semiconductor materials for UV and blue light beam devices, especially as a result of its strong eksiton tissue (~ 60 meV (Van de Walle 2001)). Eksiton is a bound state of an electron and holes are attracted to one another by using electrostatic coulomb force.

ZnO material quite fast expansion in eight years ago or some of the results of high quality, wide - area substrates grown by hydrothermal and vapor transport method - phase as well as with high - quality ZnO thin layers can be grown by various techniques such as MBE, PLD (Pulsed Laser Deposition), MOCVD and a host of others.

2. Literature Review.

The importance of the use of ZnO gas sensor was shown in 1962 to combustible gas materials[9]. ZnO gas sensors have been designed in various forms, such as single crystals[10], sintered pellets, thick layer, a thin layer, and Heterojunction. ZnO thin layer of gas is expected to exhibit a high level of sensitivity, because the detection mechanism involves chemical absorption (chemisorption) followed by charge transfer to the surface that make a difference in the resistance of the detector element.

Different methods were used to obtain a thin layer of ZnO, eg, oxidation temperature, chemical deposition, electron beam evaporation, reactive evaporation activation, spray pyrolysis, chemical vapor deposition of metal organic low pressure (MOCVD) and RF magnetron spray.

2. 1. Synthesis Of Zno Nano Chemical Structure.

ZnO occurs as white powder known as zinc white or zincite / mineral zincite. This mineral usually contains a number of elements manganese and other elements and yellow to red. ZnO crystal material is thermo-chromic material, changing from white to yellow when heated with water vapor will return to white in the cooling process. This situation caused a very small loss of oxygen at high temperatures to form a material Zn1 + XO, where the temperature is 8000C obtained, x = 0.00007.

ZnO is an amphoteric oxide, this material is virtually insoluble in water and alcohol, but it can be dissolved in acid material, such as hydrochloric acid.

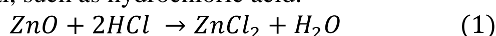

$$ZnO + 2HCl \rightarrow ZnCl_2 + H_2O \quad (1)$$

This method also remove solid material to give zincates solution;

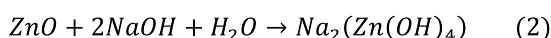

$$ZnO + 2NaOH + H_2O \rightarrow Na_2(Zn(OH)_4) \quad (2)$$

ZnO reacts slowly with fatty acids in the oil to produce the same carbocylate, such as oleate or stearate. ZnO forms cement products when mixed with a solution of the form of solid solution of zinc hydroxy chloride. This cement was used in dentistry. ZnO decomposes into zinc vapor and oxygen only at a temperature of 1975^{0}C, this shows great stability. Heating with carbon is the process of converting into steam zinc oxide;

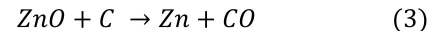

$$ZnO + C \rightarrow Zn + CO \quad (3)$$

ZnO reacts rapidly with powdered aluminum and magnesium powders, with chlorinated rubber and linseed oil on heating time cause fire and explosion. ZnO also react with hydrogen sulfide to give the sulfide: this reaction is used commercially to remove H2S to give ZnO powder (eg, use a deodorant);

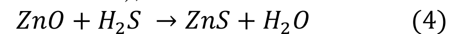

$$ZnO + H_2S \rightarrow ZnS + H_2O \quad (4)$$

When ointments containing ZnO materials and water, then diluted and exposed to UV light then the hydrogen peroxide can be produced.

2. 2. ZnO Crystal Structure.

ZnO crystallized in three forms: Wurtzite Hexagonal, Cubic Zincblende and cubical rock salt (which is rarely studied form). Wurtzite structure is the most stable and the most common confines. Zincblende form can be stabilized by increasing the ZnO on substrates with cubic lattice structure. In the second - two cases and Zinc oxide is a tetrahedron. NaCl rock salt type structure is only observed at relatively high pressure; ~ 10 GPa .

Form a hexagonal structure and zinc alloy ZnO lattice symmetry does not have an inverter (relative reflectance at every point is given crystal structure, where the point is not altered structure into ZnO structure itself). ZnO lattice and lattice other materials to produce nature - lattice symmetry in the piezoelectric properties of hexagonal structure of ZnO and zinc in the alloy and the pyro -electric properties of ZnO structures (shown in figure 1). Hexagonal structure has a point group 6 mm (note Herman - Mauguin) or C_{6V} (note Schoenflies), and space group P6$_3$ mc or C_{6V}. Lattice constants are a = 3.25 A^0 and c = 5.2 A^0, then obtained a constant ratio $c/a \sim 1.60$ suitable approach to the structure of the hexagonal cell $c/a = 1.633$. Like most of the II - VI, the bond energy of ZnO is largely ionic bond which explains that the piezoelectric material is strong .

Due to the ionic bond plane, zinc and oxygen, the ZnO material containing electric charges (positive and negative charges respectively). Therefore, to maintain the electrical charge neutrality, the plane - the plane was rebuilt atomic level in a number of materials, but not in the ZnO material: material surface atoms form a flat, stable and show the lack of reconstruction. This is an anomaly of ZnO is not fully explained.

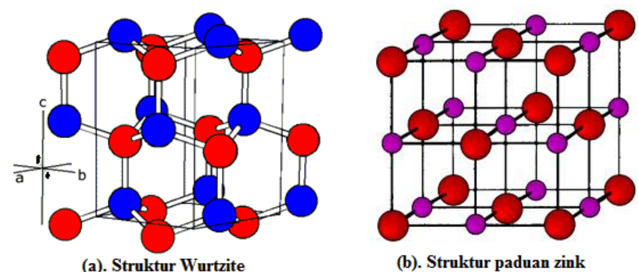

Figure 1. ZnO Crystal Structure[9].

3. Method Of Average Scanning Fast Fourier Transform (ASFFT).

Two functions of the existing discrete coefficients of the X and Y coordinate plane, ASFFT method gives an average direction (X or Y) or average - Fx and average - Fy from 1-dimensional discrete FFT data source. The following scale is provided to illustrate the method of calculation of the spectrum in the FFT and have other distinctive objectives, namely [11];

1. Power spectral density technique (SIT - or KSK X - Y).
2. Power spectrum technique (sk - x or sk - y).
3. Magnitude Spectrum technique (modulus function average-Fx or average-Fy).
4. Square root of the magnitude techniques.
5. Logarithmic Spectrum Techniques (natural or decimal) of the power spectrum.

The first peak in the average yield curve TFC can be detected, then filtered coordinate position, and length of relationship to the peak is displayed together - similar to the peak position impressed.

Average yield calculation ASFFT method with discrete Fourier transform of each segment 1D X or Y depends on the choice of direction. A part of the discrete Fourier transformation (DFT) – 1D $Fx(m, v_k)\left(Fy(m, v_q)\right)$ of the source data set $z(X_n, Y_m)$ defined on $N_x \times N_y$ partition along the to-m in the X(Y) taken as equality,

$$Fx(m, v_k) = \frac{1}{N_x}\sum_{n=0}^{N_x-1} Z(X_n, Y_m)\exp(-i2\pi X_n v_k) = \frac{1}{N_x}\sum_{n=0}^{N_x-1} Z(X_n, Y_m)\exp\left(-i2\pi\left(\frac{kn}{N_x}\right)\right) \quad (5)$$

$$Fy(n, u_q) = \frac{1}{N_y}\sum_{m=0}^{N_y-1} Z(X_n, Y_m)\exp(-i2\pi Y_m u_q) = \frac{1}{N_y}\sum_{m=0}^{N_x-1} Z(X_n, Y_m)\exp\left(-i2\pi\left(\frac{qm}{N_y}\right)\right) \quad (6)$$

which map points are assumed to have the same distance with separation L_x in X and L_y in Y directions in the form of a square size $L_x \times L_y$; volume n and m of the 1D transformation produces the range $n = 0, 1, 2, \dots N_x - 1$ and $m = 0, 1, 2, \dots N_y - 1$;

$$v_k = k\frac{1}{L_x}, \quad u_q = q\frac{1}{L_y}$$

are space frequency in X and Y direction (7)

$$\Delta v_k = \frac{1}{L_x}, \quad \Delta u_q = \frac{1}{L_y}$$

are increment frequency relationship (8)

Total segments in the X – direction of equal to the number of points on the Y – segment and so the amount of segments in the Y – direction equal to the number of points on the Z – segment. Spectrum $Fx(m, v_k)$ and $Fy(n, u_q)$ is calculated by using the ASFFT algorithm.

ASFFT spectrum is calculated with the average $Fx(m, v_k)$ or $Fy(n, u_q)$ on segments that are interconnected. In writing, the average Fourier spectrum of the X (Avg - Fx) is given by the equation:

$$Average - Fx = C_x(v_k) = \frac{1}{N_y}\sum_{m=0}^{N_y-1} Fx(m, v_k) = \frac{1}{N_y}\sum_{m=0}^{N_y-1}\frac{1}{N_x}\sum_{n=0}^{N_x-1} Z(X_n, Y_m)\exp(-i2\pi X_n v_k) \quad (9)$$

Average Fourier spectrum in the Y – direction (Avg - Fy) is given by the equation:

$$Average - Fy = C_y(u_q) = \frac{1}{N_x}\sum_{n=0}^{N_x-1} Fy(n, u_q) = \frac{1}{N_x}\sum_{n=0}^{N_x-1}\frac{1}{N_y}\sum_{m=0}^{N_y-1} Z(X_n, Y_m)\exp(-i2\pi Y_m u_q) \quad (10)$$

Second spectrum average - Fx and average - Fy are worth complexes:

$$Average - Fx = Re(Average - Fx) + i\,Im(Average - Fx) = C_x(v_k) = |C_x(v_k)|\exp(i\,arg\,C_x(v_k)) \quad (11)$$

$$Average - Fy = Re(Average - Fy) + i\,Im(Average - Fy) = C_y(u_q) = |C_y(u_q)|\exp(i\,arg\,C_y(u_q)) \quad (12)$$

where i stands for the imagination unit, Re(*) and Im(*) denotes the real and the imagination part of the argument above equation.

Average modulus spectrum for a special direction is defined as the average of the modulus of Fourier spectrum in a predetermined direction:

$$|C_x(v_k)| = |Purata - Fx| \quad (13)$$

$$|C_y(u_q)| = |Purata - Fy| \quad (14)$$

Average power spectrum (SK - X and SK - Y) is defined as the square module of the average Fourier spectrum that related:

$$SK - X = |C_x(v_k)|^2 = |Purata - Fx|^2 \quad (15)$$

$$SK - Y = |C_y(u_q)|^2 = |Purata - Fy|^2 \quad (16)$$

For the average power spectral density function (KSK - X and KSK - Y) is defined as the following equation:

$$KSK - X = \frac{|C_x(v_k)|^2}{\Delta v_k} = \frac{|C_x(v_k)|^2}{1/L_x} = \frac{KS - X}{1/L_x} \quad (17)$$

$$KSK - Y = \frac{|C_y(u_q)|^2}{\Delta v_k} = \frac{|C_y(u_q)|^2}{1/L_y} = \frac{KS - Y}{1/L_y} \quad (18)$$

4. Testing Materials.

Material testing of ZnO is performed by using scanning probe microscopy (MKP) NTEGRA AURA (NT-MDT), as can be seen in Figure 2 and 3.

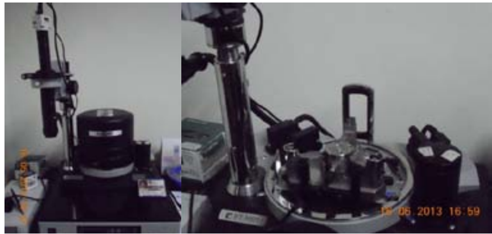

Figure 2. NTEGRA AURA scanning probe microscopy at the front view (left) and sample placement of ZnO material (right).

Figure 3. ZnO sample on the glass substrate.

Table 1. MKP NTEGRA AURA spesification.

Spesification		Scanning Type	
		using sample	using probe
Sample size		∅ upper 40mm, sample high above 15mm	∅ upper 100mm, sample high above 15mm
Sample Weight		above 100 g	above 300 g
Range of sample placement XY, resolution		5 x 5 mm, 5 µm	
Position sensitivity		2 µm	
Scanning Range		100 x 100 x 10 µm 3 x 3 x 2.6 µm	50 x 50 x 5 µm
		above 150 x 150 x 15 µm (dual-scanning modes)	
XY - nonlinearity with closed circuit detection		≤ 0.1%	≤ 0.15%
Noise level, Z (RMS on the broadband 1000 Hz).	With detector	0.04 nm (typically) ≤ 0.06 nm	0.06 nm (typically) ≤ 0.07 nm
	Without detector	0.03 nm	0.05 nm
Noise level, XY(RMS on the broadband 200 Hz).	With detector	0.2 nm(typically) ≤0.3nm(XY100 um)	0.1 nm (typically) ≤ 0.2 nm
	Without detector	0.02 nm (XY 100 um) 0.001 nm (XY3 um)	0.01 nm
Close Loop Equivalence	XY Noise Level (RMS on the broadband 200 Hz)	0.012 nm (XY 3 um)	
	Z Noise Level (RMS on the broadband 1000 Hz)	0.02 nm	
	Zoom Accuracy	5% (typically)	
Optical View System	Optical resolution	1 um	3 um
	Viewing Area	4.5 – 0.4 mm	2.0 – 0.4 mm
	Zoom Continuity	Available	Available
Thermal Control	Range	from RT until +150^{0}C	
	Stability	±0.005^{0}C (typically), ≤ ±0.01^{0}C	
Vacuum System	Pressure	10^{-2} Torr	
Vibration Isolation	Active	0.7 – 1000 KHz	
	Passive	Up to 1 KHz	

The following figure is the result of SPM scanning tested on ZnO material by placing the material on a glass substrate. Stipulation of ZnO on the substrate material designed to see surface features and surface roughness

Figure 4 below taken at the shooting range as large as 3.336 um of surface. Shooting distance is calculated based on scanning probe tip distance and ZnO sample material, as illustrated in Figure 5.13.

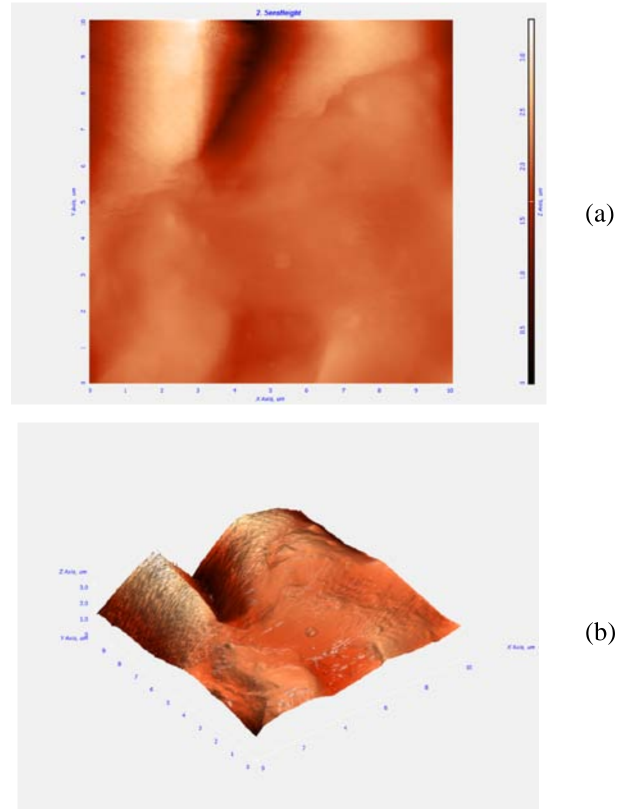

Figure 4. ZnO samples with wide of 10 x 10 x 3.336 um; (a). Results for 2-D image (b). Results for the 3-D image.

Figure 5 below shows that the scanner is located at the cantilever tip. Appropriate probe tip will move to the surface of the material being tested. This means using the tip of scanning has been used extensively in the Atomic Force Microscopy (AFM), which was created in 1986 by Gerd Binnig, Calvin F. Morton and Christopher Herber [10].

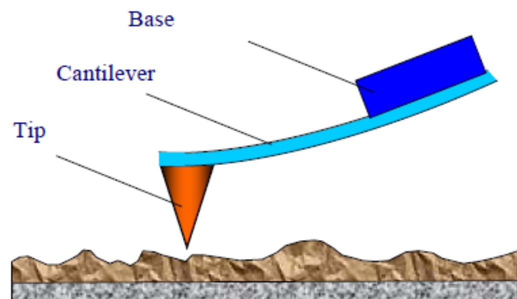

Figure 5. Probe tip of AFM [9].

The function of AFM is interactivity force measurement between the measurement probe tip and the material surface using a special probe made of an elastic cantilever with a sharp tip. Force applied to the tip of the probe by the surface is the result of the bending of the cantilever.

Measurement of cantilever bending, we can get the interactivity value of material surface.

With an atomic force microscope, it can study the detailed characteristic description of the interaction of local force, as well as receiving information about the nature of the sample surface. This goal is called as the distance curve of the atomic force (the tip will approach to or withdraw from the sample surface). Actually, the tip movement of the cantilever bending ΔZ (as a result of this movement is the interaction force) on the z – axis which is existed at a distance of sample investigation. Form of ΔZ = f (z) is shown in Figure 6.

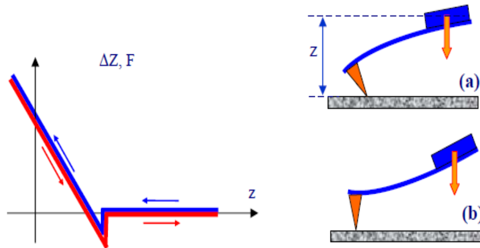

Figure 6. Schematic ΔZ cantilever deflection (proportional to the F – force) over a distance z-probe. Blue-line : Approachment, Red-line : puller back [9].

In the approach to the end surface of the probe gain traction. It causes the bending of the cantilever to the sample surface (Figure 6, in part (a)). Probe tip jumps to the surface due to the gradient of charm close to the sample surface. For this type of attraction Lennard - Jones Z*, which gradient $F_z{}'$ high, around 1 nanometer.

Competitive behavior of Lennard - Jones and derivatives with respect to the tip distance and the surface are shown schematically in Figure 7.

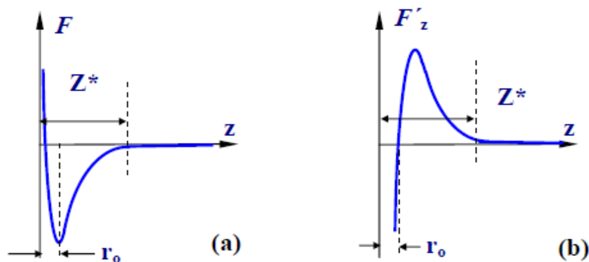

Figure 7. Figure of force schematic (a) and force of slope as distance function of *z* between probe tip and material surface (b).

Probe tip jumps to the material surface can be examined only when the elastic constant of the cantilever is very small than maximum gradient force. This can be explained by considering the motion equations of an elastic cantilever close to the material surface to be tested:

$$m\ddot{z}_1 = -kz_1 + F(d + z_1) \qquad (19)$$

Where d is the probe tip distance of the surface material in a state of equilibrium and z_1 is displacement from equilibrium position. $F(z)$ is the interaction force tip surface material, k and m are the elastic constants and the mass of the cantilever. By using a linear approximation of the function $F(z)$, we get the equation,

$$F = F(d) + F'_z(d) \cdot z_1 \qquad (20)$$

$$mz''_1 + [k - F'_z(d)]z_1 = F(d) \qquad (21)$$

with replacement, $z_2 = z_1 - \frac{F(d)}{k - F'_z(d)}$, motion equation take to the form:

$$z''_2 + {\omega_0}^2 z_2 = 0 \qquad (22)$$

$${\omega_0}^2 = \frac{k - F'_z(d)}{m} \qquad (23)$$

This form, explaining that oscillator frequency of ω_0, depending on the distance. If the force slope is greater distance from the elastic constants of the cantilever, then ${\omega_0}^2 < 0$. This situation corresponds to an unstable equilibrium position of an inverted pendulum. Any small disturbance results from the loss of stability and the cantilever will move to the material surface.

In the probe approaches to the material sample, the probe tip begins to experience the repulsion power and the cantilever bends in the opposite direction (Figure 7, insert (b)). Slope curve ΔZ = f(z) is determined by two samples of the elastic properties and cantilever . If a perfectly elastic interaction, dependence on distance curve is recorded during reverse motion, in accordance with the dependence obtained during forward motion (Figure 6) . For soft sample material (plastic) , such as material - organic , biological structures, and others - others, as well as for samples with adsorbed layers of various materials, the curves ΔZ = f (z) is complex . In this case, the curve shape is influenced by capillary effects and the elasticity impact.

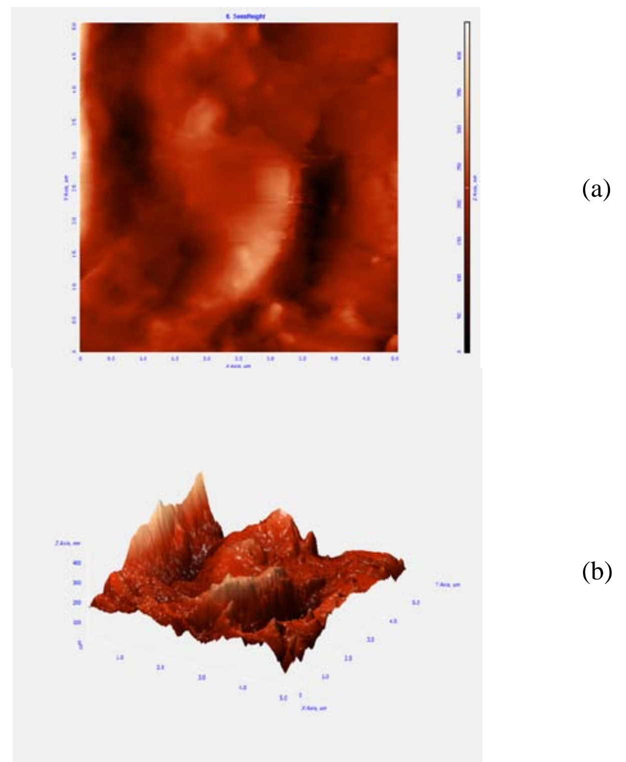

(a)

(b)

Figure 8. ZnO samples with size area 5 um x 5 um x 443.1 nm; (a). Image result in 2-D; (b). Image result in 3-D.

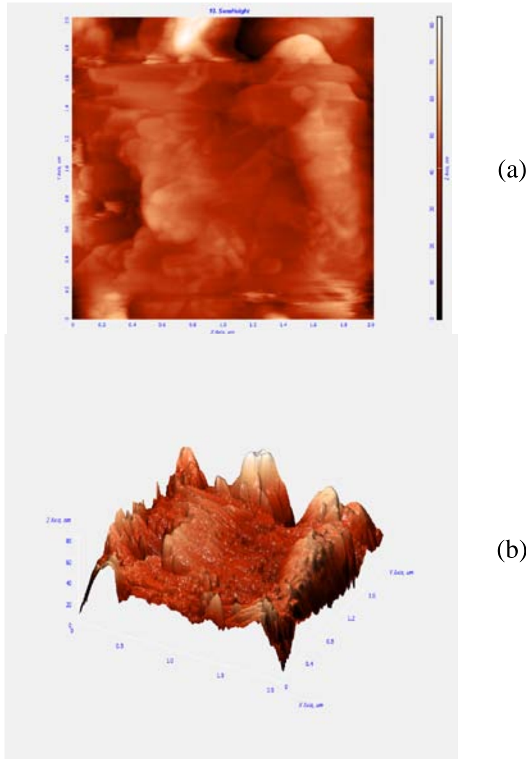

(a)

(b)

Figure 9. ZnO samples with size area 2 um x 2 um x 82.1 nm; (a). Image result in 2-D; (b). Image result in 3-D.

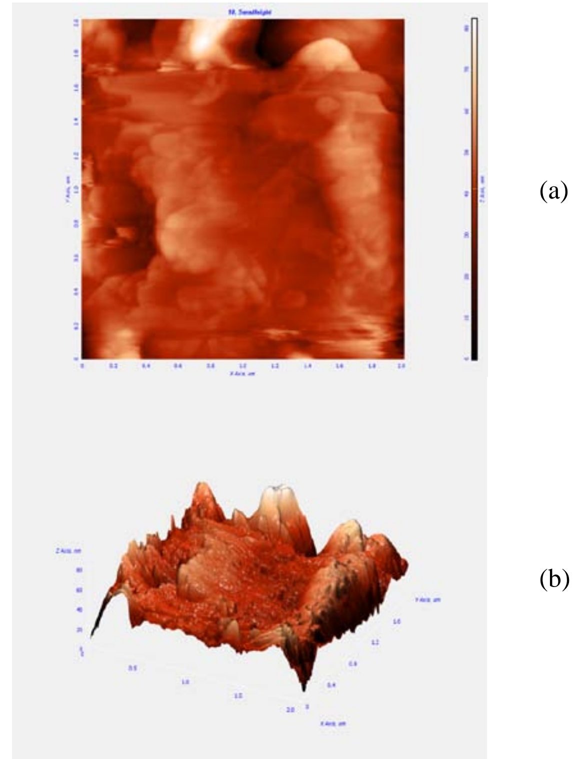

(a)

(b)

Figure 11. ZnO samples with size area 50 um x 50 um x 16.35 um; (a). Image result in 2-D; (b). Image result in 3-D.

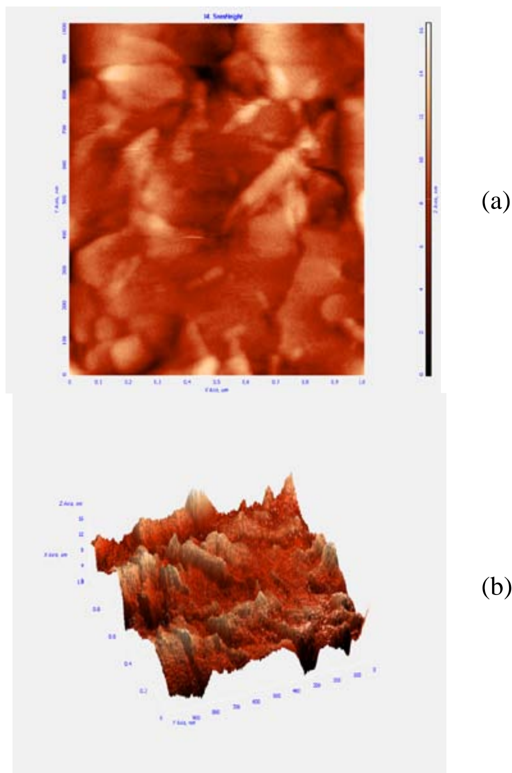

(a)

(b)

Figure 10. ZnO samples with size area 1 um x 1 um x 16.31 nm;(a). Image result in 2-D; (b). Image result in 3-D.

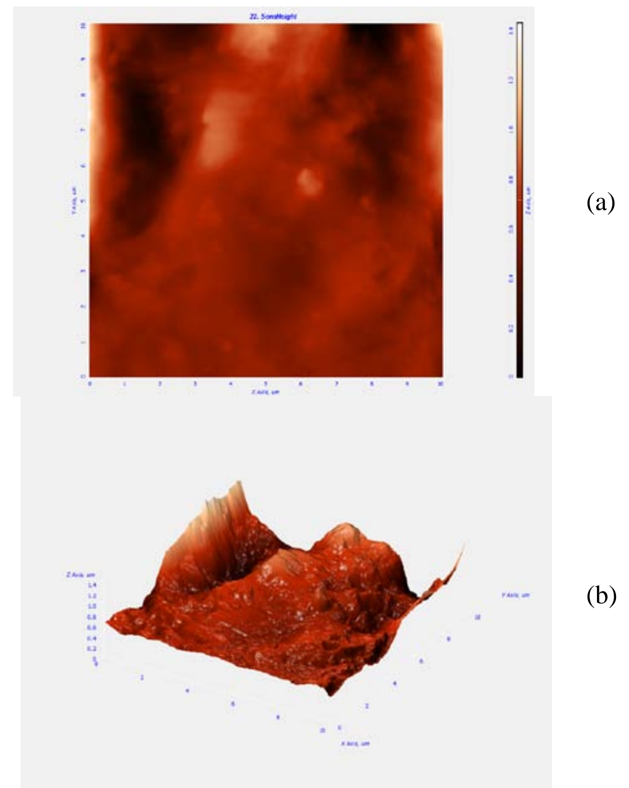

(a)

(b)

Figure 12. ZnO samples with size area 10 um x 10 um x 1.4 um; (a). Image result in 2-D; (b). Image result in 3-D.

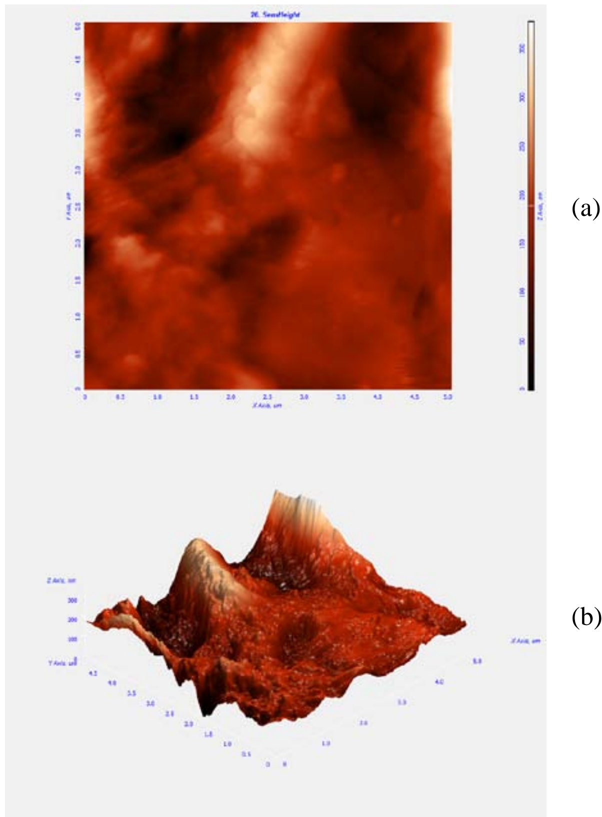

Figure 13. ZnO samples with size area 5 um x 5 um x 376.8 nm; (a). Image result in 2-D; (b). Image result in 3-D.

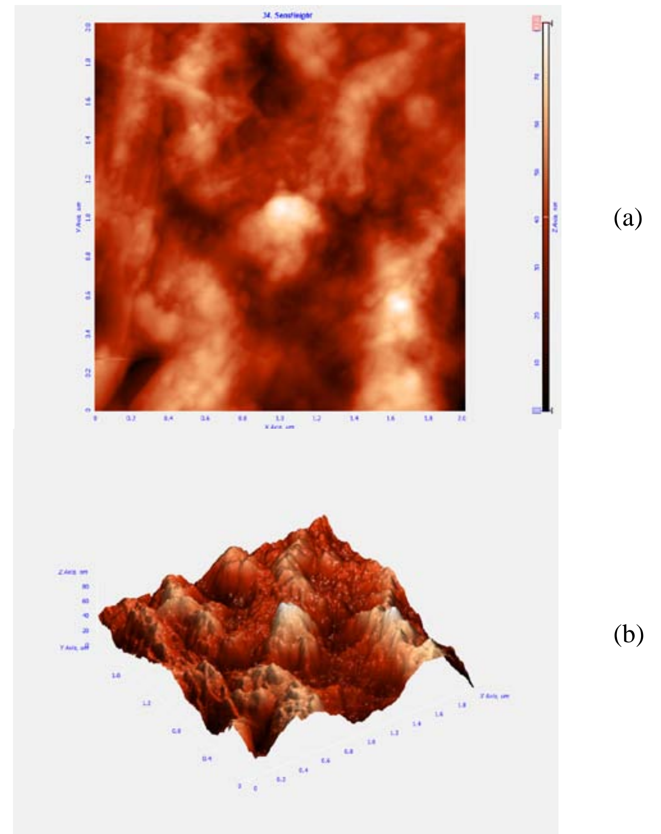

Figure 15. ZnO samples with size area 2 um x 2 um x 81.0 nm; (a). Image result in 2-D; (b). Image result in 3-D.

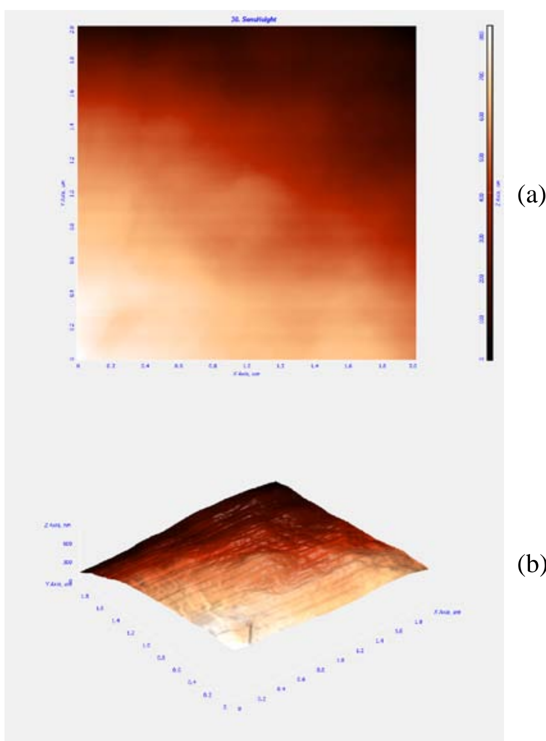

Figure 14. ZnO samples with size area 2 um x 2 um x 822 nm; (a). Image result in 2-D; (b). Image result in 3-D.

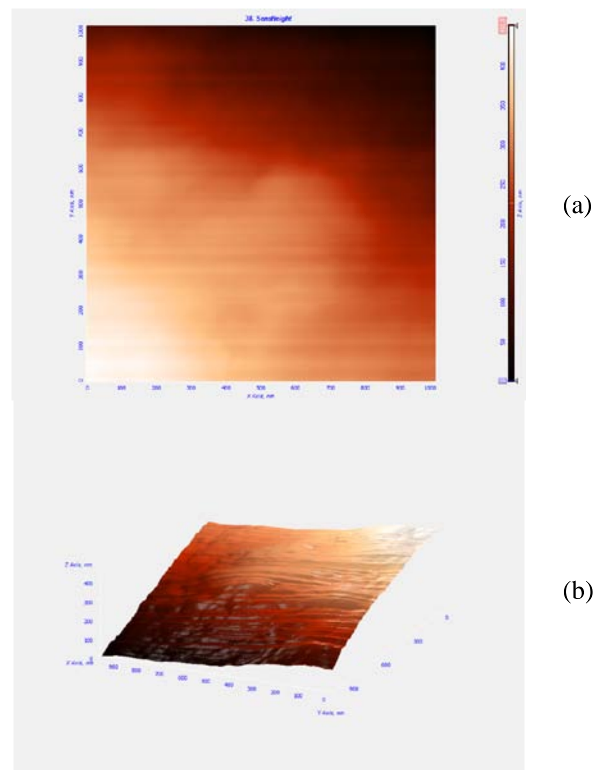

Figure 16. ZnO samples with size area 1 um x 1 um x 451 nm;(a). Image result in 2-D; (b). Image result in 3-D.

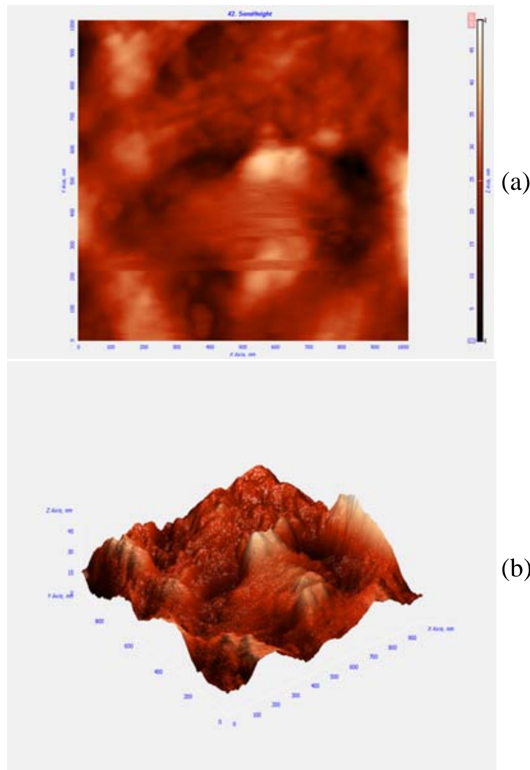

Figure 17. ZnO samples with size area 1 um x 1 um x 49.49 nm; (a). Image result in 2-D; (b). Image result in 3-D.

5. Result Experiment And Discussion Of ASFFT Method.

Micro – scale surface morphology determines the various phenomena that are important for fundamental science and technological applications. In this part of the study will be explained based on the ASFFT method that it has been determined. ASFFT method goal is to change the function of the tip distance variable observations into normal function or frequency variable. Each scaling results will be seen ASFFT measurement of the maximum peak of dominant position by TFC spectrum in units of um, the probe tip position error in units of um, Peak dominant position by the smoothed spectrum in units of um and an average value for each technique TFC; Maximum Power Spectrum Density, maximum power spectrum, spectrum modulus, maximum magnitude spectrum and Maximum logarithmic spectrum.

5. 1. Power Spectral Density Technique.

Table 2 is the simulation results that obtained from a scanning test of ZnO material. Reduction of parameters are utilized for this simulation is the average reduction, it was exploited to determine the source of the data preprocessing. The average data sources are applied in the past by using the average TFC. Simulation results can be seen from the simulation based discrete functions of two variables X and Y axis fields, for the table 2 and table 3 data generated from X – direction and Y – direction.

In the third column of table 1 is the volume of a sample of observations from the simulation results. It is determined to compare againts the maximum power spectral density for the results of this comparison can distinguish and observe of FFT scaling characterization methods.

Table 2. Simulation Result using *Image Analysis P9* with FFT Scalling for Power Spectrum Density in X – direction.

No	Size of observation sample	Volume of Observation Sample (um^3)	FFT Scalling : Power Spectrum Density			
			Dominant Peak Position of FFT Spectrum (um)	Position Error (um)	Peak Position Dominant of Smoothed Spectrum (um)	Maximum of Power Spectrum Density
1	10 um x 10 um x 3.336 um	333.6	0.09255	0.000858	0.09223	0.00000000004241 um*um^2
2	5 um x 5 um x 443.1 nm	11.0775	0.04612	0.0004337	0.04627	0.000009760 um*nm^2
3	2 um x 2 um x 82.1 nm	0.3284	0.01979	0.0001989	0.01947	0.000003515 um*nm^2
4	1 um x 1 um x 16.31 nm	0.01631	0.1115	0.01154	0.1135	0.000002094 um*nm^2
5	50 um x 50 um x 16.35 um	40875	1.4341	0.03938	1.4331	0.00000000009554 um*um^2
6	10 um x 10 um x 1.4 um	140	0.1209	0.001499	0.001499	0.00000000002582 um*um^2
7	5 um x 5 um x 376.8 nm	9.42	0.04239	0.0003547	0.04201	0.00001083 um*nm^2
8	2 um x 2 um x 822 nm	3.288	0.1056	0.005237	0.1057	19079.9612 um*nm^2
9	2 um x 2 um x 81.0 nm	0.324	0.02321	0.0002767	0.02305	0.000003654 um*nm^2
10	1 um x 1 um x 451 nm	0.451	0.1003918	0.0091265	0.1004552	2467515.7072 nm*nm^2
11	1 um x 1 um x 49.49 nm	0.04949	0.0456326	0.001984	0.046.1818	0.001006 nm*nm^2

Table 3. Simulation Result using *Image Analysis P9* with FFT Scalling for Power Spectrum Density in Y – direction

No	Size of observation sample	Volume of Observation Sample (um^3)	FFT Scalling : Power Spectrum Density			
			Dominant Peak Position of FFT Spectrum (um)	Position Error (um)	Peak Position Dominant of Smoothed Spectrum (um)	Maximum of Power Spectrum Density
1	10 um x 10 um x 3.336 um	333.6	0.09255	0.000858	0.09223	0.00000000004241 um*um^2
2	5 um x 5 um x 443.1 nm	11.0775	0.04612	0.0004337	0.04627	0.000009760 um*nm^2
3	2 um x 2 um x 82.1 nm	0.3284	0.01979	0.0001989	0.01947	0.000003515 um*nm^2
4	1 um x 1 um x 16.31 nm	0.01631	0.1115	0.01154	0.1135	0.000002094 um*nm^2
5	50 um x 50 um x 16.35 um	40875	1.4341	0.03938	1.4331	0.00000000009554 um*um^2
6	10 um x 10 um x 1.4 um	140	0.1209	0.001499	0.001499	0.00000000002582 um*um^2
7	5 um x 5 um x 376.8 nm	9.42	0.04239	0.0003547	0.04201	0.00001083 um*nm^2

8	2 um x 2 um x 822 nm	3.288	0.1056	0.005237	0.1057	19079.9612 um*nm^2
9	2 um x 2 um x 81.0 nm	0.324	0.02321	0.0002767	0.02305	0.000003654 um*nm^2
10	1 um x 1 um x 451 nm	0.451	0.1003918	0.0091265	0.1004552	2467515.7072 nm*nm^2
11	1 um x 1 um x 49.49 nm	0.04949	0.0456326	0.001984	0.046.1818	0.001006 nm*nm^2

Figure 18 shows FFT results from the specimen material of surface morphology into surface frequency of material.The data of surface morphology is available from the result scanning based on distance intensity domain of Atomic Force Microscopy (AFM).

The graphs below explains the data about of power spectral density value in the frequency domain. Preliminary data can be seen from the results of the processing of Image Analysis software P9 (IA-P9) as shown in figure 4, 8, 9, 10, 11, 12, 13, 14, 15, 16 and 17. Range frequency domain obtained starting at 0.0000 1/um to 0.5000 1/um. This range frequency shows the maximum value of IA-P9 simulation.

Figure 20 exposes that peak value of power spectral density is very low, it indicates that occur thinning observation layer of ZnO material and has a flat surface morphology.

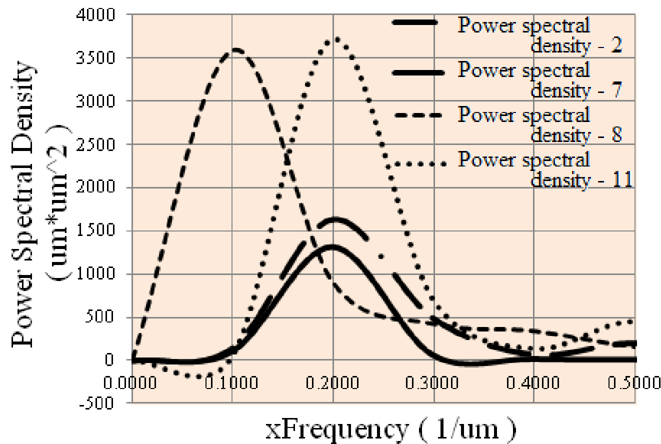

Figure 18. Simulation result of power spectrum density in X – direction on the appropriate figure 8 (Power Spectral Density 2), figure 13 (Power Spectral Density 7), figure 14 (Power Spectral Density 8) figure 17 ((Power Spectral Density 11).

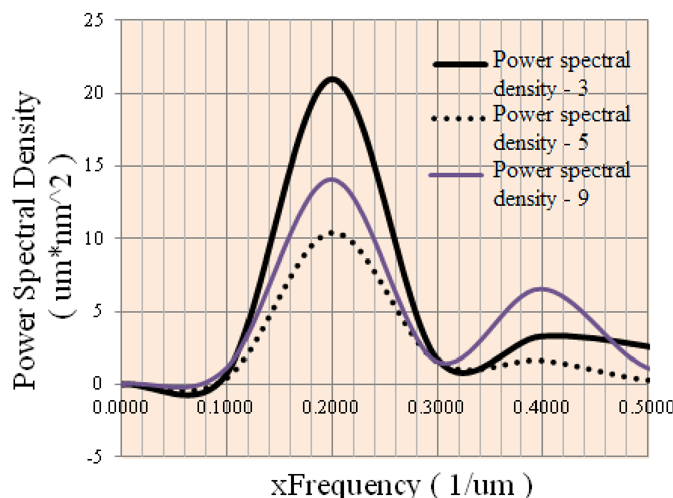

Figure 19. Simulation result of power spectrum density in X – direction on the appropriate figure 9 (Power Spectral Density 3), figure 11 (Power Spectral Density 5), figure 15 (Power Spectral Density 9).

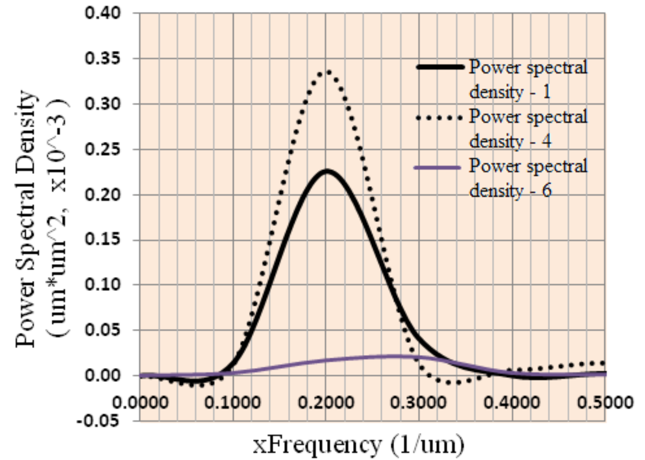

Figure 20. Simulation result of power spectrum density in x – direction on the appropriate figure 4 (power spectral density 1), figure 10 (power spectral density 4), figure 12 (power spectral density 6).

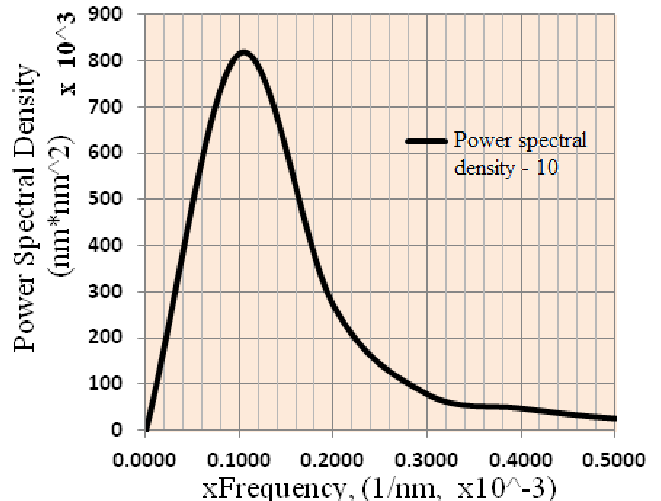

Figure 21. Simulation result of power spectrum density in X – direction on the appropriate figure 16 (Power Spectral Density 10).

5. 2. Power Spectral Technique.

Power spectral technique is a quadratic process of material surface spectrum from data resources of fourier spectral. It is acquired from simulation and measurement result from Atomic Force Microscopy (AFM). Simulation result is seen into two circumstances namely; x-axis and y-axis. Situation of power spectral technique could be watched on material surface morphology with difference of distance observation.

Table 4 describes simulation result of FFT – Scaling for power spectral on the x – direction and y – direction. These result are seen according to the data obtained based on sample size of ZnO. Simulation results provide some data of peak dominant position by FFT spectrum in μm unit, errror position in μm, peak dominant position by the smoothed spectrum in μm unit and power spectral maximum.

Table 4. Simulation result using *Image Analysis P9* with FFT Scalling for Power Spectrum in X – direction.

Directivity		: X Fourier				
Decrement		: Average				
No	Size of observation sample	Volume of Observation Sample (um^3)	FFT Scalling: Power Spectrum			
			Dominant Peak Position of FFT Spectrum (um)	Position Error (um)	Peak Position Dominant of Smoothed Spectrum (um)	Maximum of Power Spectrum
1	10 um x 10 um x 3.336 um	333.6	5.0196	1.6732	5.0457	0.02284 um^2
2	5 um x 5 um x 443.1 nm	11.0775	2.5098	0.8366	2.6928	326.0563 nm^2
3	2 um x 2 um x 82.1 nm	0.3284	1.0039	0.3346	0.9254	10.4250 nm^2
4	1 um x 1 um x 16.31 nm	0.01631	0.5019	0.1673	0.4758	0.3344 nm^2
5	50 um x 50 um x 16.35 um	40875	25.098	8.366	23.5294	0.2063 um^2
6	10 um x 10 um x 1.4 um	140	3.3464	0.8366	3.2549	0.002006 um^2
7	5 um x 5 um x 376.8 nm	9.42	2.5098	0.8366	2.6535	261.1490 nm^2
8	2 um x 2 um x 822 nm	3.288	0.01693	0.0001301	0.01693	1785.6925 nm^2
9	2 um x 2 um x 81.0 nm	0.324	1.0039	0.3346	1.0562	7.0021 nm^2
10	1 um x 1 um x 451 nm	0.451	0.0092955	0.0000858	0.009295	811.6331 nm^2
11	1 um x 1 um x 49.49 nm	0.04949	0.5019604	0.1673201	0.436601	3.7110 nm^2

Table 5. Simulation Result using *Image Analysis P9* with FFT Scalling for Power Spectrum in X – direction.

Directivity		: Y Fourier				
Decrement		: Average				
No	Size of observation sample	Volume of Observation Sample (um^3)	FFT Scalling: Power Spectrum			
			Dominant Peak Position of FFT Spectrum (um)	Position Error (um)	Peak Position Dominant of Smoothed Spectrum (um)	Maximum of Power Spectrum
1	10 um x 10 um x 3.336 um	333.6	0.09255	0.000858	0.09223	0.000000000004276 um^2
2	5 um x 5 um x 443.1 nm	11.0775	0.04612	0.0004337	0.04627	0.000001975 nm^2
3	2 um x 2 um x 82.1 nm	0.3284	0.01979	0.0001989	0.01947	0.000001787 nm^2
4	1 um x 1 um x 16.31 nm	0.01631	0.1115	0.01154	0.1135	0.000002016 nm^2
5	50 um x 50 um x 16.35 um	40875	1.4341	0.03938	1.4331	0.000000000001836 um^2
6	10 um x 10 um x 1.4 um	140	0.1209	0.001499	0.1211	0.000000000002583 um^2
7	5 um x 5 um x 376.8 nm	9.42	0.04239	0.0003547	0.04201	0.000002086 nm^2
8	2 um x 2 um x 822 nm	3.288	0.1056	0.005237	0.1057	9502.7177 nm^2
9	2 um x 2 um x 81.0 nm	0.324	0.02321	0.0002767	0.02305	0.000001756 nm^2
10	1 um x 1 um x 451 nm	0.451	0.1003918	0.0091265	0.1004552	2457.8786 nm^2
11	1 um x 1 um x 49.49 nm	0.04949	0.0456326	0.001984	0.0461818	0.000001064 nm^2

In the table 4, the simulation results can be seen to get the maximum power spectral in nm^2. In accordance with the basic function of FFT is change the height of the surface morphology domain into the frequency domain. Power spectrum – 3, power spectrum – 9 and power spectrum – 11 on the figure 22, there are the power spectrum amount of 10.4250 nm^2, 7.0022 nm^2, and 3.7110 nm^2 respectively. All the power spectrums have a surface frequency amount 0.1992 1/um.

It occurs because the material surface morphology in the inhomogeneous condition, as well as the peaks of power spectral in each sample. Inhomogeneous condition of the material due to different observation area that is made by AFM.

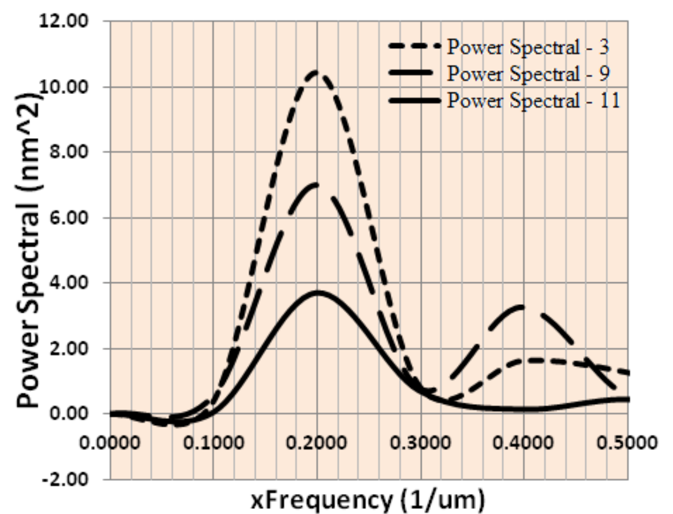

Figure 22. Simulation result of power spectrum in x - direction on the appropriate figure 9 (Power Spectrum - 3), figure 15 (Power Spectrum - 9) and figure 17 (Power Spectrum - 11).

Figure 23 shows the maximum line of power spectral – 10 can be found at 811.6331 nm^2 at surface frequency of 0.0996 1/um and power spectral – 8 shows the maximum line is 1785.6925 nm^2 at surface frequency 0.0996 1/um. Comparing to figure 24, 25, 26, simulation result from figure 23 is more homogenous and more wide of spectrum.

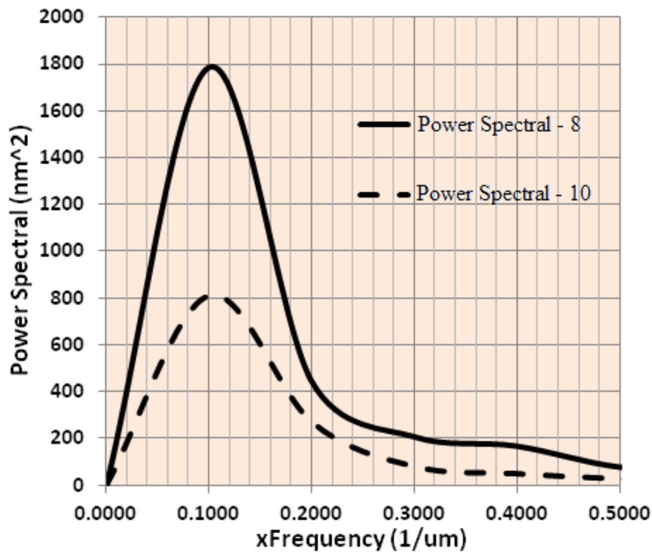

Figure 23. Simulation result of power spectrum in x - direction on the appropriate figure 14 (Power Spectrum - 8) and figure 16 (Power Spectrum - 10)

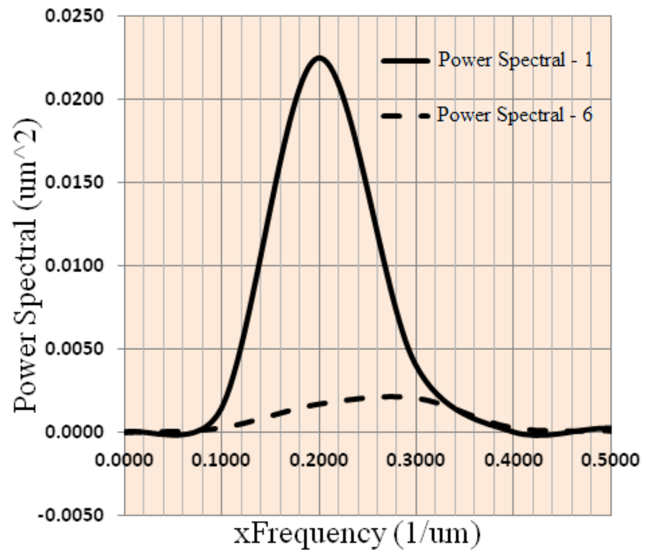

Figure 26. Simulation result of power spectrum in x-direction on the appropriate figure 4 (Power Spectrum – 1) and Figure 12 (Power Spectrum – 6)

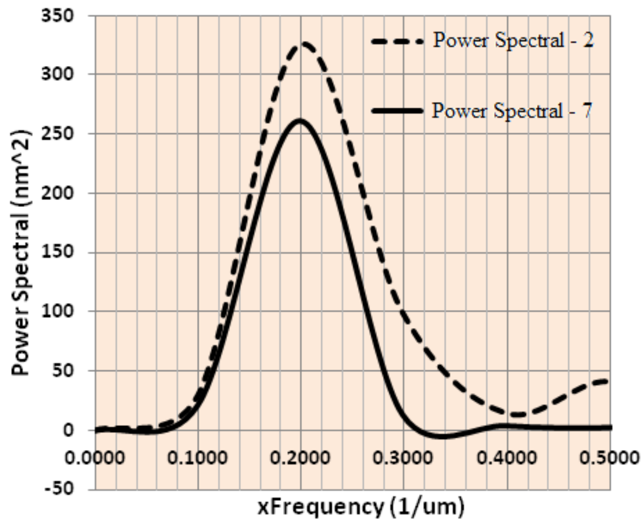

Figure 24. Simulation result of power spectrum in x - direction on the appropriate figure 8 (Power Spectrum - 2) and figure 13 (Power Spectrum - 7)

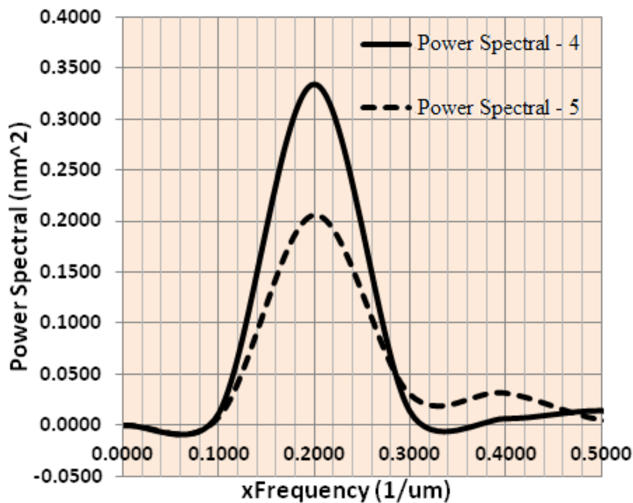

Figure 25. Simulation result of power spectrum in x – direction on the appropriate figure 10 (Power Spectrum - 4) and figure 11 (Power Spectrum - 5).

5. 3. Magnitude Spectral Technique.

Magnitude spectrum technique is known as spectral modulus or modulus of the average fourier spectrum. This technique derived from the squares of the power spectrum in 5.5.2. Dominant position spectrum is created by FFT, error and peak position of dominant that it have same smoothed spectral outcomes.

Maximum of magnitude value can be seen from simulation analysis results on the Table 6 for x – direction and Table 7 for y – direction. The unit of maximum magnitude value is nanometer (nm) and it is given for distance of high observation level in each difference AFM captures. Maximum of spectral magnitude is founded amount 42.2574 nm with X – direction and 97.4818 nm with Y – direction.

FFT method is known as frequency domain of images cause capture lines represent of sinusoidal wave part. In random frequency domain, each lines have amplitude value that saved on the uncoordinate location of X and Y, but they are recorded based on frequency of X and Y. These coordinate are digital image views while frequency will define as small doubler or frequency unit and pixel coordinate that represent to index or double integer unit of frequency. This condition occurs from rule of coordinate function that running continously, then it can be delegated with combination of sinusoidal wave. On the other hand, representation of frequency domain is one way to save and open the image from space domain.

Pixel size can be wide or large of high image level. For consent to centralize image that proper from the origin FFT, it requires an even-dimension. This condition is take place after applies inversion of fourier transformation, so that image need to reproduce into the origin dimension for pitch out the store of space. Fourier transform consist of complex number causes transformation cannot observe directly. Magnitude spectral is one of image component from modification of complex number.

Table 6. Simulation result using *Image Analysis P9* with FFT scalling for Magnitud Spectrum in X – direction.

Directivity		: X Fourier				
Decrement		: Average				
			FFT Scalling : Modulus Spectral (Magnitude)			
No	Size of observation sample	Volume of Observation Sample (um^3)	Dominant Peak Position of FFT Spectrum (um)	Position Error (um)	Peak Position Dominant of Smoothed Spectrum (um)	Magnitude Maximum (nm)
1	10 um x 10 um x 3.336 um	333.6	5.0196	1.6732	5.0457	149.9
2	5 um x 5 um x 443.1 nm	11.0775	2.5098	0.8366	2.6928	18.0570
3	2 um x 2 um x 82.1 nm	0.3284	1.0039	0.3346	0.9254	3.2287
4	1 um x 1 um x 16.31 nm	0.01631	0.5019	0.1673	0.4758	0.5782
5	50 um x 50 um x 16.35 um	40875	25.098	8.366	23.5294	454.3
6	10 um x 10 um x 1.4 um	140	3.3464	0.8366	3.2549	45.23
7	5 um x 5 um x 376.8 nm	9.42	2.5098	0.8366	2.6535	16.1601
8	2 um x 2 um x 822 nm	3.288	0.01693	0.0001301	0.01693	42.2574
9	2 um x 2 um x 81.0 nm	0.324	1.0039	0.3346	1.0562	2.6461
10	1 um x 1 um x 451 nm	0.451	0.0092955	0.0000858	0.009295	28.4891
11	1 um x 1 um x 49.49 nm	0.04949	0.5019604	0.1673201	0.436601	1.9264

Table 7. Simulation result using *Image Analysis P9* with FFT scalling for Magnitud Spectrum in Y – direction.

Directivity		: Y Fourier				
Decrement		: Average				
			FFT Scaling : Modulus Spectral (Magnitude)			
No	Size of observation sample	Volume of Observation Sample (um^3)	Dominant Peak Position of FFT Spectrum (um)	Position Error (um)	Peak Position Dominant of Smoothed Spectrum (um)	Magnitude Maximum (nm)
1	10 um x 10 um x 3.336 um	333.6	0.09255	0.000858	0.09223	0.002036
2	5 um x 5 um x 443.1 nm	11.0775	0.04612	0.0004337	0.04627	0.001355
3	2 um x 2 um x 82.1 nm	0.3284	0.01979	0.0001989	0.01947	0.001337
4	1 um x 1 um x 16.31 nm	0.01631	0.1115	0.01154	0.1135	0.001447
5	50 um x 50 um x 16.35 um	40875	1.4341	0.03938	1.4331	0.001361
6	10 um x 10 um x 1.4 um	140	0.1209	0.001499	0.1211	0.001569
7	5 um x 5 um x 376.8 nm	9.42	0.04239	0.0003547	0.04201	0.001482
8	2 um x 2 um x 822 nm	3.288	0.1056	0.005237	0.1057	97.4818
9	2 um x 2 um x 81.0 nm	0.324	0.02321	0.0002767	0.02305	0.001300
10	1 um x 1 um x 451 nm	0.451	0.1003918	0.0091265	0.1004552	49.5769
11	1 um x 1 um x 49.49 nm	0.04949	0.5019604	0.1673201	0.436601	1.9264

Figure 27, 28, 29 and 30 are likely different than figure 23, 24, 25 and 26 because there are broad spectrum and many peaks spectral. Frequency value obtained amount of 0.3984 (1/um).

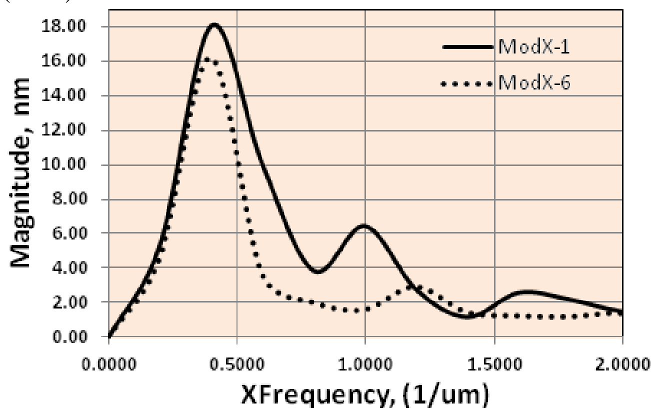

Figure 27. Simulation result of magnitude spectrum of x-direction in frequency domain that appropriate with figure 4(ModX-1) and figure 12(ModX-6).

Figure 28 states that many spectrals peak from the data of ModX-2, ModX -3, ModX -8, ModX -11 and ModX -9. This condition explains that material sample have uneven of surface morphology.

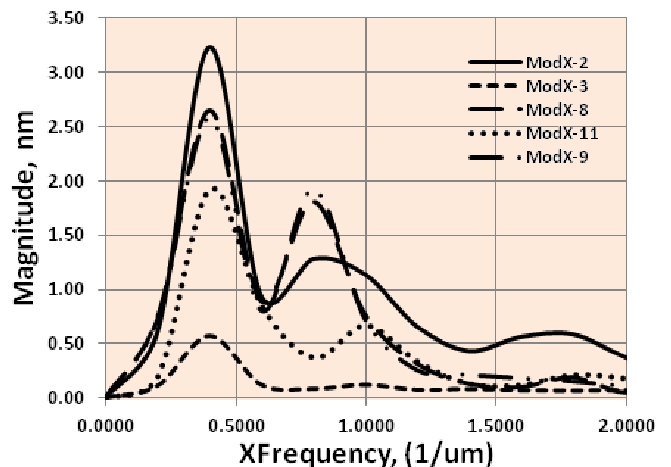

Figure 28. Simulation result of magnitude spectrum of x-direction in frequency domain that appropriated with figure 8(ModX-2), figure 9(ModX-3), figure 14(ModX-8) figure 17(ModX-11) dan figure 15(ModX-9).

frequency range of x-coordinate at power spectrum amount of 0.500, it is given because simulation result shows the other low peak value. Different spectral case that any most significant value. Figure 28, there are peak value of spectrum that most significant compared with main peak value of spectrum. It is shown at the simulation result of image at ModX-2, ModX-8 and ModX-2.

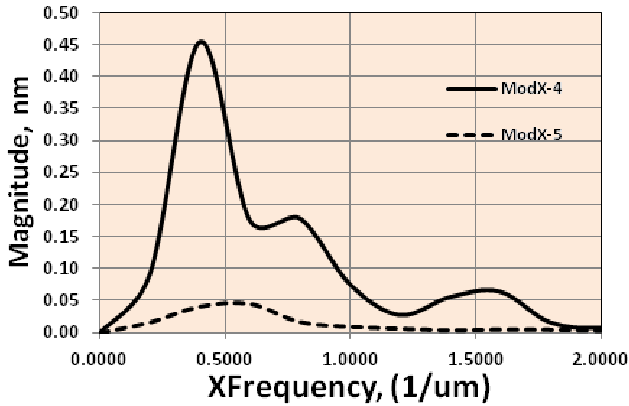

Figure 29. Simulation result of magnitude spectrum of x-direction in frequency domain that appropriated with figure 10 (ModX - 4) and figure 11 (ModX - 5).

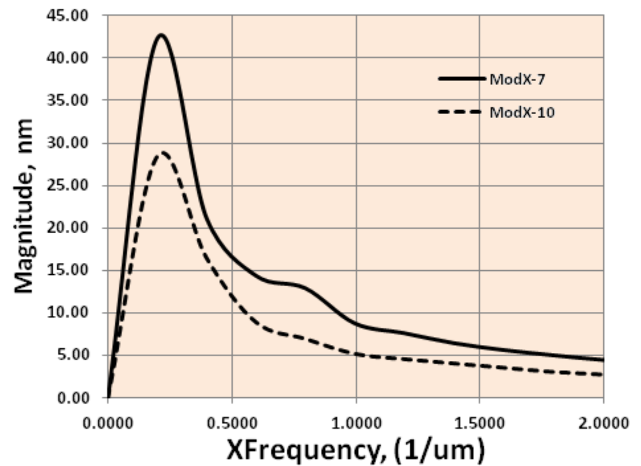

Figure 30. Simulation result of magnitude spectrum of x-direction in frequency domain that appropriated with figure 13 (ModX – 7) and figure 16 (ModX - 10).

Figure 29 exposes that comparison between two different image of surface morphology ZnO material. ModX-5 is more flat than ModX-4 and also the surface layer is more thin.

If we see this case that exposed from figure 30, we can get conclusion that sample of materials are checked by AFM microscope. It have thick layer with the flat material morphology. The surface thickness can be seen from the slope of a line graph over ramps and different from other image samples.

This part only gives an explaination about simulation result for x-direction where y-direction gives lowest value. Simulation result of x-direction gives the same meaning with scanning result of x-direction, likewise with y-direction.

5. 4. Square Root Magnitude Spectral Technique

This technique is one of AS-FFT scanning method. The square root magnitude spectral creates the value from magnitude spectral at section 5.3. Measurement result is obtained from the probe tip until surface of material sample.

Table 8 and 9 shows simulation result of surface morphology that produced by AFM, where the spectral technique as a maximum result of square root magnitude spectrum with unit of (um)1/2. Both of tables performs the different maximum value of square root magnitude amounted 0.6740000 (um^1/2) with the dominant peak position value is 25.098 um, and also 0.3122180 (um^1/2) with the dominant peak position value is 0.1056 um. These values refers from figure 11 and 14, it can be resulted from capture image of microscope (AFM).

Table 8. Simulation result using *Image Analysis P9* with FFT scaling for square root of the magnitude spectrum in x-direction.

Directivity		: X Fourier				
Decrement		: Average				
			FFT Scalling : Square root of the magnitude			
No	Size of observation sample	Volume of Observation Sample (um^3)	Dominant Peak Position of FFT Spectrum (um)	Error Position (um)	Peak position dominant of smoothed spectrum (um)	Maximum of square root of the magnitude spectrum (um^1/2)
1	10 um x 10 um x 3.336 um	333.6	5.0196	1.6732	5.0457	0.3872000
2	5 um x 5 um x 443.1 nm	11.0775	2.5098	0.8366	2.6928	0.1343747
3	2 um x 2 um x 82.1 nm	0.3284	1.0039	0.3346	0.9254	0.0568198
4	1 um x 1 um x 16.31 nm	0.01631	0.5019	0.1673	0.4758	0.0240460
5	50 um x 50 um x 16.35 um	40875	25.098	8.366	23.5294	0.6740000
6	10 um x 10 um x 1.4 um	140	3.3464	0.8366	3.2549	0.2138000
7	5 um x 5 um x 376.8 nm	9.42	2.5098	0.8366	2.6535	0.1271204
8	2 um x 2 um x 822 nm	3.288	0.01693	0.0001301	0.01693	0.2055639
9	2 um x 2 um x 81.0 nm	0.324	1.0039	0.3346	1.0562	0.0514408
10	1 um x 1 um x 451 nm	0.451	0.0092955	0.0000858	0.009295	0.1687866
11	1 um x 1 um x 49.49 nm	0.04949	0.5019604	0.1673201	0.436601	0.0438893

Table 9. Simulation result using *Image Analysis P9* with FFT scaling for square root of the magnitude spectrum in y-direction

Directivity		: Y Fourier				
Decrement		: Average				
			FFT Scalling : Square root of the magnitude			
No	Size of observation sample	Volume of Observation Sample (um^3)	Dominant Peak Position of FFT Spectrum (um)	Error Position (um)	Peak position dominant of smoothed spectrum (um)	Maximum of square root of the magnitude spectrum (um^1/2)
1	10 um x 10 um x 3.336 um	333.6	0.09255	0.000858	0.09223	0.0014300
2	5 um x 5 um x 443.1 nm	11.0775	0.04612	0.0004337	0.04627	0.0011881
3	2 um x 2 um x 82.1 nm	0.3284	0.01979	0.0001989	0.01947	0.0011444

4	1 um x 1 um x 16.31 nm	0.01631	0.1115	0.01154	0.1135	0.0011742
5	50 um x 50 um x 16.35 um	40875	1.4341	0.03938	1.4331	0.0011300
6	10 um x 10 um x 1.4 um	140	0.1209	0.001499	0.1211	0.0012970
7	5 um x 5 um x 376.8 nm	9.42	0.04239	0.0003547	0.04201	0.0011776
8	2 um x 2 um x 822 nm	3.288	0.1056	0.005237	0.1057	0.3122180
9	2 um x 2 um x 81.0 nm	0.324	0.02321	0.0002767	0.02305	0.0011403
10	1 um x 1 um x 451 nm	0.451	0.1003918	0.0091265	0.1004552	0.2226560
11	1 um x 1 um x 49.49 nm	0.04949	0.0456326	0.001984	0.0461818	0.0010309

Figure 31 shows four square root of the magnitude spectrum has frequency or the frequency spectrum amounted 0.1992 1/um, with the magnitude of 0.7605 um^1/2, 0.6740 um^1/2, 0.3872 um^1/2 and 0.2138 um^1/2.

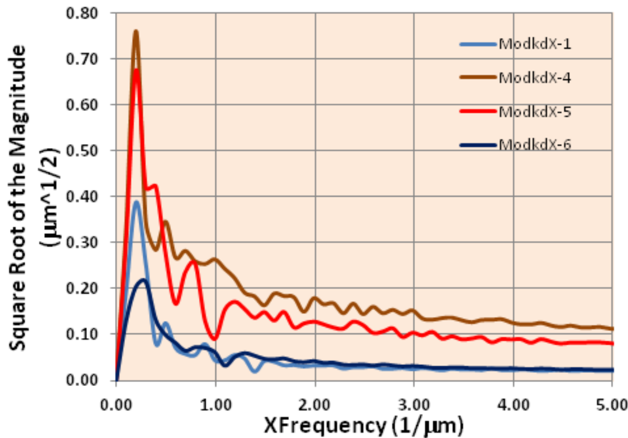

Figure 31. Simulation result of square root of the magnitude in x- direction that appropriated with figure 4 (ModkdX – 1), figure 10 (ModkdX - 4), Figure 11 (ModkdX - 5) and Figure 12 (ModkdX - 6).

Figure 32 pointed the difference of line graph as like as modkdX-10 and modkdX-8 compared to the other samples. First, it provides the information that the image captured by a microscope on a flat surface morphology of ZnO. Second, the material samples of ModkdX–8 and ModkdX–10 have thickness that is different; it can be seen from the square root of the magnitude maximum.

Figure 32 also shows the frequency spectrum for each distinct maximum value of the square root of the magnitude. The line graphs of ModkdX-2 and ModkdX-7 have the square root magnitude equal to 0.1992 (um^1 / 2) while the other line of ModkdX-8 and ModkdX-10 have the square root of the magnitude equal to 0.0996 (um^1/2). This also applies the same magnitude in figure 33 on the line graph (ModkdX-3, ModkdX-9, and ModkdX-11).

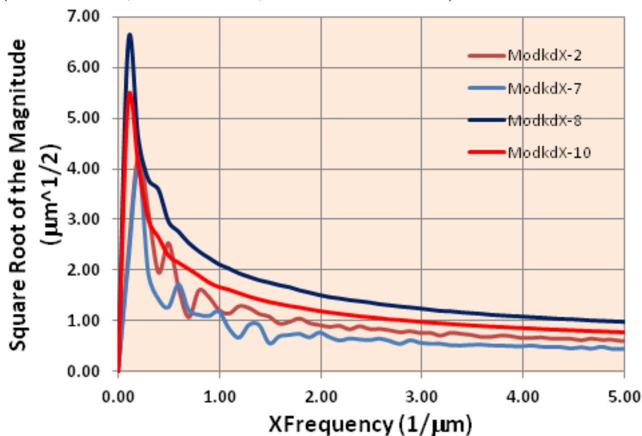

Figure 32. Simulation result of square root of the magnitude in x- direction that appropriated with figure 8 (ModkdX – 2) figure 13 (ModkdX - 7), figure 14 (ModkdX - 8) and figure 16 (ModkdX - 10).

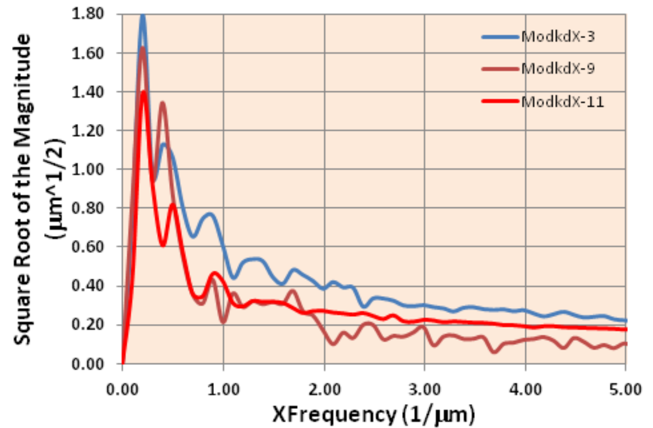

Figure 33. Simulation result of square root of the magnitude in x- direction that appropriated with figure 9 (ModkdX – 3) figure 15 (ModkdX - 9) and figure 17 (ModkdX - 11).

Figure 33 informs about non-horizontal morphology situation of ZnO layer as shown in the line graph of modkX – 3, modkX – 9 and modkX – 11, it can be seen at second and third peak spectrum. In modkX-9, the different value between first and second peak is small compared with modkX-3 and modkX-11.

5. 5. Logarithmic Spectral Technique.

Logarithmic spectral scaling technique produces value of maximum power logarithmic spectral in ln(um) unit. The aim of logarithmic power spectral is extend of dark pixel value from images when it occur the highest value of image compression. Secondly, image compression is obtained by AFM that existed at dynamic range with the variety of largest pixel value.

Logarithmic spectral technique has variety of intensity that started from 0 until 10^6 or more. This technique cannot be seen from degree of detail significantly from the image because it will disappear at the display. This result simulation is shown in table 11. Logarithmic value of maximum power spectral is origin value of logarithmic from maximum power spectral in X-direction and table 12 for Y-direction. Table 11 gives the lowest value amounted 0.002084 ln(um) with dominant peak position of FFT spectrum is 3.3464 um and the highest value is 11.232150 ln(um) or 7.4881 ln(um) with dominant peak position of FFT spectrum amounted 0.01693 um.

At the scaling of logarithmic spectrum, the image from AFM can be compressed by changing of each pixel value. It has impression that the low intensity of pixel values can be more enhanced. Frequency domain value of FFT is 0.1992 (1/um), the prevailing value in the calculation results shown at figure 4, 8, 9, 10, 12, 13, 14, 15 and 17. On the other hand, frequency value of FFT amounted 0.0996 (1/um). It can be found from calculation result of figure 16 and value of 0.2988(1/um) obtained from calculation at figure 11.

Table 10. Simulation result of *Image Analysis P9* with FFT scaling
for logarithmic spectrum in x-direction.

Directivity		: X Fourier				
Decrement		: Average				
			FFT scaling : Logarithmic Power Spectral			
No	Size of observation sample	Volume of Observation Sample (um^3)	Dominant Peak Position of FFT Spectrum (um)	Error Position (um)	Peak Position Dominant of Smoothed Spectrum (um)	Maximum power of logarithmic spectrum
1	10 um x 10 um x 3.336 um	333.6	5.0196	1.6732	5.0457	0.02234 ln(um)
2	5 um x 5 um x 443.1 nm	11.0775	2.5098	0.8366	2.6928	5.7901 ln(nm)
3	2 um x 2 um x 82.1 nm	0.3284	1.0039	0.3346	0.9254	2.4358 ln(nm)
4	1 um x 1 um x 16.31 nm	0.01631	0.5019	0.1673	0.4758	0.2885 ln(nm)
5	50 um x 50 um x 16.35 um	40875	25.0980	8.3660	23.5294	0.1876 ln(um)
6	10 um x 10 um x 1.4 um	140	3.3464	0.8366	3.2549	0.002084 ln(um)
7	5 um x 5 um x 376.8 nm	9.42	2.5098	0.8366	2.6535	5.5689 ln(nm)
8	2 um x 2 um x 822 nm	3.288	0.01693	0.0001301	0.01693	7.4881 ln(nm)
9	2 um x 2 um x 81.0 nm	0.324	1.0039	0.3346	1.0562	2.0797 ln(nm)
10	1 um x 1 um x 451 nm	0.451	9.2955	0.08580	9.2950	6.7002 ln(nm)
11	1 um x 1 um x 49.49 nm	0.04949	501.9604	167.3201	436.6010	1.5499 ln(nm)

Table 11. Simulation result of *Image Analysis P9* with FFT scaling
for logarithmic spectrum in Y-direction

Directivity		: Y Fourier				
Decrement		: Average				
			FFT scaling : Logarithmic Power Spectrum			
No	Size of observation sample	Volume of Observation Sample (um^3)	Dominant Peak Position of FFT Spectrum (um)	Error position (um)	Peak Position Dominant of Smoothed Spectrum (um)	Maximum power of logarithmic spectrum
1	10 um x 10 um x 3.336 um	333.6	0.09255	0.0008580	0.09223	0.000000000004276 ln(um)
2	5 um x 5 um x 443.1 nm	11.0775	0.04612	0.0004337	0.04627	0.000001975 ln(nm)
3	2 um x 2 um x 82.1 nm	0.3284	0.01979	0.0001989	0.01947	0.000001787 ln(nm)
4	1 um x 1 um x 16.31 nm	0.01631	0.1115	0.01154	0.1135	0.000002016 ln(nm)
5	50 um x 50 um x 16.35 um	40875	1.4341	0.03938	1.4331	0.000000000001836 ln(um)
6	10 um x 10 um x 1.4 um	140	0.1209	0.001499	0.1211	0.000000000002583 ln(um)
7	5 um x 5 um x 376.8 nm	9.42	0.04239	0.0003547	0.04201	0.000002086 ln(nm)
8	2 um x 2 um x 822 nm	3.288	0.1056	0.005237	0.1057	9.1594 ln(nm)
9	2 um x 2 um x 81.0 nm	0.324	0.02321	0.0002767	0.0002767	0.000001756 ln(nm)
10	1 um x 1 um x 451 nm	0.451	0.1003918	0.0091265	0.1004552	7.8074 ln(nm)
11	1 um x 1 um x 49.49 nm	0.04949	0.0456326	0.0019840	0.0461818	0.000001064 ln(nm)

Based on many figures below, the characterization techniques have been discussed, it can not be differentiated significantly. Dominant peak point located at 0.20 (1/um) for the frequency domain.

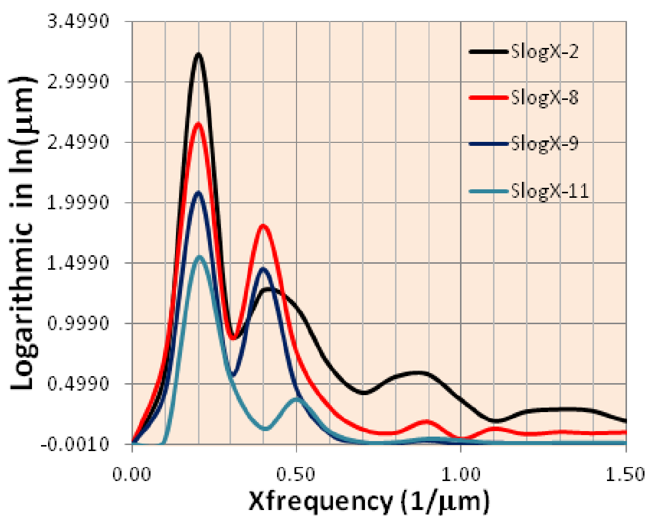

Figure 34. Simulation result of logarithmic spectrum in X – direction that appropriated with figure 8 (SlogX – 2), figure 14 (SlogX – 8) figure 15 (SlogX – 9) and figure 17 (SlogX – 11).

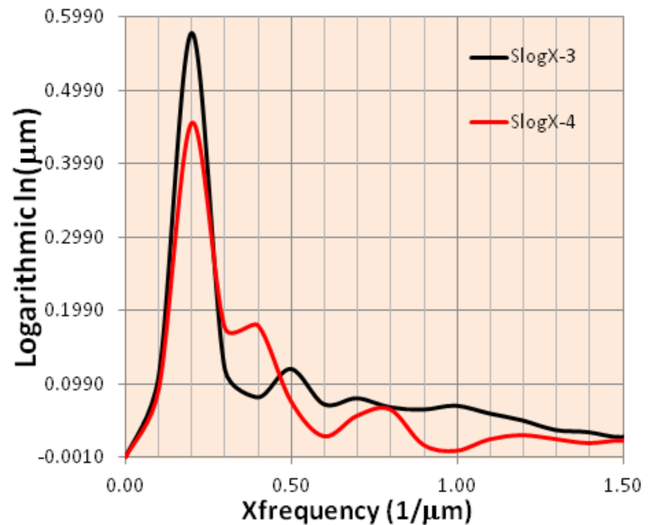

Figure 35. Simulation result of logarithmic spectrum in X-direction that appropriated with figure 9 (SlogX – 3) and figure 10 (SlogX – 4).

Figure 36 shows larger logarithmic value than the other calculation results. Logarithmic result is amount 16.1601 ln(mm) for dominant peak point. The difference of first peak value, second peak and the next peak have significant disparity. If the graph is produced as image measurement result from AFM then peak value is called the image compression.

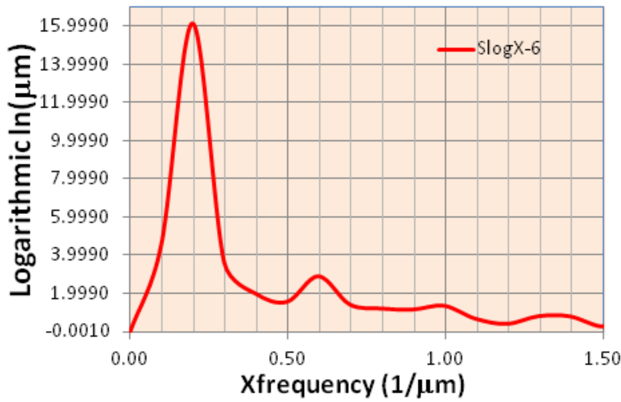

Figure 36. Simulation result of logarithmic spectrum in x – direction that appropriated with figure 12 (SlogX – 6).

We have discussed that logarithmic transformation technique to the image will extend the low rate to the high rate stage of pixel and it has some effects to high pixel rate where peak value can be defined as a point of image. Small points of image will occur caused the other peaks logarithmic around 0.60 (1/um).

Figure 37 and 38 shows the difference surface forms at three image sampel. SlogX-1, SlogX-5, SlogX-10 and SlogX-7 gives the difference dominant peak position result with 0.2(1/um), 0.27(1/um) and 0.1(1/um), 0.19(1/um) respectively. SlogX-1 gives information about image of AFM with the flat layer, if compared with SlogX-5, SlogX-10 and SlogX-7. Surface of image explains the flat condition if the spectrum line have one peak dominant position.

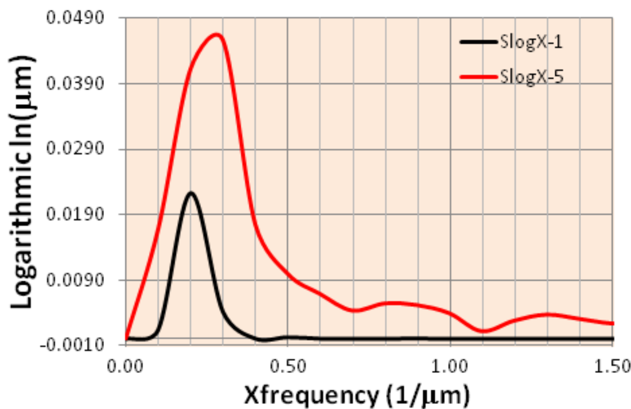

Figure 37. Simulation result of logarithmic spectrum in x – direction that appropriated with figure 4 (SlogX – 1) and figure 11 (SlogX - 5).

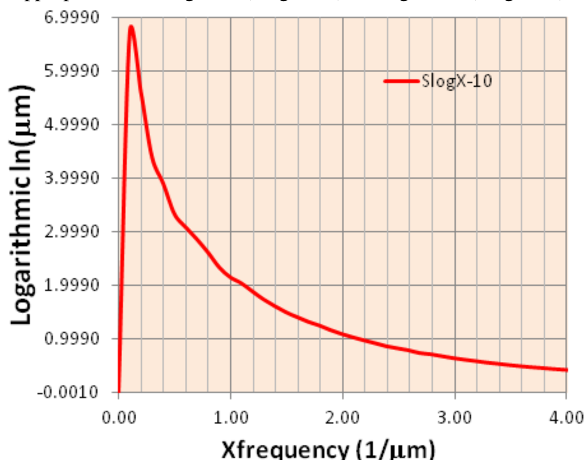

Figure 38. Simulation result of logarithmic spectrum in x – direction that appropriated with figure 16 (SlogX – 10).

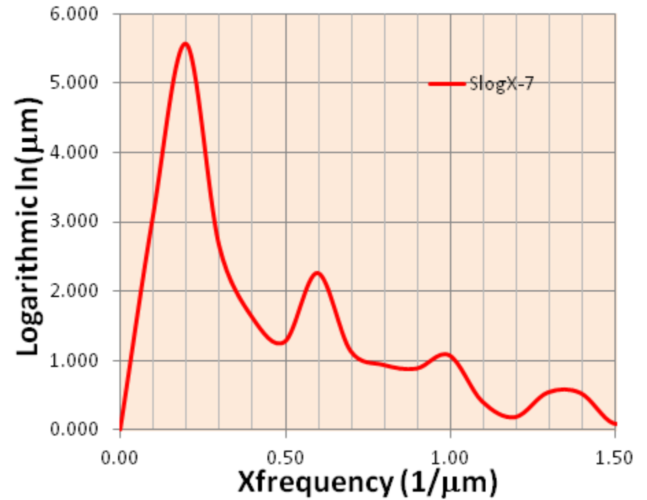

Figure 39. Simulation result of logarithmic spectrum in x – direction that appropriated with figure 13 (SlogX – 7).

In particular condition, figure 39 describes image sample from AFM with high level unhomogenity. Decline of surface level based on frequency illustrates material sample of ZnO has high level homogenity and it does not have the blank space on the ZnO material surface. Different argument in SlogX-1 that ZnO surface material deposition transpired on the exclusive location.

6. Conclusion.

The main aims of ZnO characterization process are created and tested the procedure of process, calculate and combine of the maximum of power spectral density, the maximum of power spectral, the maximum of magnitude spectral, the square root maximum of the magnitude and logarithmic spectral from Scanning Probe Microscopy that gained from the difference of z-axis scale or called as difference of mycroscope observation scale from optical surface effect.

These procedures of microscope observation have been used to examine the surface morphology of sample with eleven positions that obtained from AFM or atomic force types. This type provides more thorough understanding rather than the effect of film morfology and may assist in adjustment of deposition parameters following surface morphology requirements. The data of AFM can assisted the optimum process with purposes to reduce of random disadvantages in thin layer of optical cladding.

Figure 18, 19, 20 and 21 shows the each data can accept ZnO material that it has the difference surface morphology or can be called as the unhomogenous ZnO layer. Unhomogenous simulation result of ZnO layer represent of many cases, as like as, scratched specimen, the difference of dip time of specimens and difference observation position from microscope.

References

[1] J. Ebothe, A. E. Hichou, P. Vautrot, and M. Addou, "Flow rate and interface roughness of zinc oxide thin films deposited by spray pyrolysis technique," *Journal of Applied Physics,* vol. 93, pp. 632-640, 2003.

[2] M. Sumiya, S. Fuke, A. Tsukazaki, K. Tamura, A. Ohtomo, M. Kawasaki, and H. Koinuma, "Quantitative control and detection of heterovalent impurities in ZnO thin films grown by pulsed laser deposition," *Journal of Applied Physics,* vol. 93, pp. 2562-2569, 2003.

[3] K.-H. Bang, D.-K. Hwang, and J.-M. Myoung, "Effects of ZnO buffer layer thickness on properties of ZnO thin films deposited by radio-frequency magnetron sputtering," *Applied Surface Science,* vol. 207, pp. 359-364, 2003.

[4] M. Fujita, N. Kawamoto, T. Tatsumi, K. Yamagishi, and Y. Horikoshi, "Molecular beam epitaxial growth of ZnO on Si substrate using ozone as an oxygen source," *Japanese Journal of Applied Physics, Part 1: Regular Papers and Short Notes and Review Papers,* vol. 42, pp. 67-70, 2003.

[5] D. C. Look, "Recent advances in ZnO materials and devices," *Materials Science and Engineering: B,* vol. 80, pp. 383-387, 2001.

[6] P. R. Emtage, "The physics of zinc oxide varistors," *Journal of Applied Physics,* vol. 48, pp. 4372-4384, 1977.

[7] R. Einzinger, "Grain junction properties of ZnO varistors," *Applications of Surface Science,* vol. 3, pp. 390-408, 1979.

[8] L. F. Lou, "Current-voltage characteristics of ZnO-Bi_2O_3 heterojunction," *Journal of Applied Physics,* vol. 50, pp. 555-558, 1979.

[9] V. L. Mironov, *Fundamentals of scanning probe microscopy*, 1 ed. Nizhniy Novgorod: The Russian Academy of Sciences, Institute For Physics of Microstructures, 2004.